Structure and Functional Expression of a Member of the Low Voltage–Activated Calcium Channel Family

Tuck Wah Soong, Anthony Stea, Connie D. Hodson, Stefan J. Dubel, Steven R. Vincent, Terry P. Snutch*

Oscillatory firing patterns are an intrinsic property of some neurons and have an important function in information processing. In some cells, low voltage–activated calcium channels have been proposed to underlie a depolarizing potential that regulates bursting. The sequence of a rat brain calcium channel α_1 subunit (rbE-II) was deduced. Although it is structurally related to high voltage–activated calcium channels, the rbE-II channel transiently activated at negative membrane potentials, required a strong hyperpolarization to deinactivate, and was highly sensitive to block by nickel. In situ hybridization showed that rbE-II messenger RNA is expressed in regions throughout the central nervous system. The electrophysiological properties of the rbE-II current are consistent with a type of low voltage–activated calcium channel that requires membrane hyperpolarization for maximal activity, which suggests that rbE-II may be involved in the modulation of firing patterns.

In the nervous system, voltage-dependent Ca^{2+} channels regulate the rapid entry of Ca^{2+} into cells and mediate a variety of physiological effects, including neurotransmitter release and the generation and control of neuronal firing patterns (*1*). Calcium channels represent a diverse class of molecules that traditionally have been grouped into two major categories according to their kinetics and voltage-dependent properties (*2*). High voltage–activated (HVA) Ca^{2+} channels first activate upon depolarization to relatively positive potentials and display diverse kinetics, pharmacologies, and sensitivities to voltage (N-, L-, and P-types). The HVA Ca^{2+} channels are multisubunit complexes, including a large, pore-forming α_1 subunit that encodes many of the unique electrophysiological and pharmacological properties of these channels (*3*, *4*). The four classes of Ca^{2+} channel α_1 subunits identified to date in the mammalian central nervous system (classes A, B, C, and D) are components of HVA Ca^{2+} channels (*4*, *5*).

Low voltage–activated (LVA) Ca^{2+} channels are available for opening only from negative membrane holding potentials and transiently activate with small depolarizations (*2*, *6*). The electrical properties of LVA Ca^{2+} channels (also called T-type channels) have led to proposals for their roles in the mediation of pacemaking activity, repetitive bursting, and secretion (*1*, *7*). Some LVA Ca^{2+} channels have been identified as targets of anticonvulsants, and dysfunction of LVA Ca^{2+} channels has been implicated in some forms of epileptiform activity (*8*). Various low-threshold Ca^{2+} conductances have been described that differ with respect to kinetics, voltage dependence, and pharmacology, which suggests that structurally distinct forms of LVA Ca^{2+} channels exist. We describe here the primary structure, localization, and functional characteristics of a rat brain Ca^{2+} channel α_1 subunit that is structurally related to the HVA class A and B proteins but displays many of the properties described for a subset of LVA Ca^{2+} channels in neurons.

We used the polymerase chain reaction (PCR) and molecular cloning to identify a new class of rat brain Ca^{2+} channel α_1 subunit (rbE-II) (*9*). The first in-frame ATG of rbE-II is followed by a 6666-bp open reading frame encoding a protein of 2222 amino acids with a predicted molecular mass of 252 kD (Fig. 1). Similar to sequences found in other cloned Ca^{2+} channel α_1 subunits (*4*, *5*), the deduced amino acid sequence of rbE-II consists of four mainly hydrophobic domains (I through IV); each domain has regions that are predicted to be transmembrane α helices (S1 through S6) (Fig. 1). Comparison with other classes of rat brain Ca^{2+} channel α_1 subunits (*10*) revealed that rbE-II is more closely related to the class A and class B proteins (53 to 54% amino acid identity) than to the α_1 subunits encoding L-type Ca^{2+} channels (~23% overall identity to rbC and rbD). The conserved sequences between rbE-II and the rbA-I and rbB-I proteins are not equally distributed but are concentrated in the four hydrophobic domains and the first, ~170 amino acids past S6 of domain IV (Fig. 1). Of particular interest, both the highly hydrophilic segments separating domains II and III and the COOH-terminal region of rbE-II show little conservation of primary sequence among the neuronal Ca^{2+} channel α_1 subunits. These two regions contain many potential sites for phosphorylation by several different protein kinases and may reflect portions of rbE-II that are targets of modulation.

The functional properties of rbE-II were determined by transient expression in *Xenopus laevis* oocytes (*11*). Depolarization from a holding potential of −100 mV resulted in macroscopic barium currents (I_{Ba}) that activated rapidly [time constant (τ) = 2.1 ± 0.1 ms; n = 65] and decayed significantly (τ = 99.6 ± 4.2 ms; n = 65) during depolarized test potentials (Fig. 2A). The current-voltage relation for rbE-II in 4 mM Ba^{2+} showed that I_{Ba} first activated at −50 mV and peaked around −10 mV (Fig. 2B). The mean amplitude of the peak I_{Ba} induced in oocytes by rbE-II was 565.5 ± 51.7 nA (n = 71), ranging from 80 to 2100 nA. The rapid decay of the rbE-II I_{Ba} was unlike the decay of that in both L- and P-type Ca^{2+} channels but similar to that found for some N-type Ca^{2+} channels (*2*). However, compared to that in N-type Ca^{2+} channels, the rbE-II I_{Ba} activated at more hyperpolarized potentials (−50 to −10 mV), values generally in the range of those found in LVA Ca^{2+} channels (*12*).

The sensitivity of rbE-II to pharmacological agents shown to interact with defined HVA Ca^{2+} channels was examined. Both the L-type Ca^{2+} channel agonist Bay K 8644 (10 μM; n = 8) (Fig. 2C) and antagonist nifedipine (10 μM; n = 6) had no significant effect on the rbE-II I_{Ba}. Similarly, the N-type Ca^{2+} channel peptide toxin, ω-conotoxin GVIA (ω-CgTx-GVIA) (1 μM; n = 6), had little effect on rbE-II (Fig. 2D). At a concentration of the funnel-web spider peptide toxin, ω-agatoxin IVA (ω-Aga-IVA), shown to completely block P-type Ca^{2+} channels (200 nM), the rbE-II I_{Ba} was only partially blocked (33 ± 6.2%, n = 8) (Fig. 2E). Furthermore, unlike the effect of ω-Aga-IVA on P-type Ca^{2+} channels (*13*), the inhibition of the rbE-II I_{Ba} did not reverse with the application of several short depolarizing pulses. Thus, consistent with its electrophysiological characteristics, the pharmacological profile of rbE-II is also distinct from that of the HVA L-, N-, and P-type Ca^{2+} channels.

Although the pharmacology of LVA Ca^{2+} channels is poorly defined, they can generally be distinguished by a marked sensitivity to Ni^{2+}. The rbE-II subunit was highly sensitive to block by Ni^{2+} (Fig. 2F). A dose-response curve determined the 50% inhibition concentration (IC_{50}) for Ni^{2+} to be 28 μM. However, unlike some types of LVA Ca^{2+} channels, rbE-II was also potently blocked by Cd^{2+} (>80% block by 10 μM Cd^{2+}; n = 7). The rbE-II I_{Ba} was insensitive to octanol (100 μM; n = 5) and only slightly inhibited by 1 mM amiloride (16.4 ± 6.2%; n = 7). Taken together, the properties of rbE-II appear to define a class of LVA Ca^{2+} channels.

Biotechnology Laboratory and Departments of Psychiatry and Zoology, University of British Columbia, Vancouver, British Columbia, Canada V6T 1Z3.

*To whom correspondence should be addressed.

Several studies examining the functional properties of cloned Ca^{2+} channel α_1 subunits have found that co-expression with a Ca^{2+} channel β subunit results in modulation of a number of kinetic and voltage-dependent properties (*14*). To explore this, we examined the effect of co-expression of a cloned rat brain β subunit (β_1) with rbE-II (*15*). Co-expression of rbE-II and β_1 did not significantly alter the magnitude of the whole cell current (655 ± 118.6 nA; n = 29) or the rate of activation (τ = 2.4 ± 0.2 ms; n = 25) but caused a shift in the current-voltage relation to more negative potentials. Activation curves fitted to normalized currents showed that the voltage at which one-half of the rbE-II I_{Ba} was activated ($V_{1/2}$) was −24.6 ± 0.7 mV (n = 21), whereas co-expression of rbE-II and β_1 shifted $V_{1/2}$ to −29.1 ± 0.7 mV (n = 12; P < 0.001) (Fig. 3A). A further major effect of the β_1 subunit was on the voltage dependence of inactivation of rbE-II. The prepulse potential at which one-half of the maximal rbE-II I_{Ba} was inactivated shifted from −65.2 ± 1.1 mV (n = 17) to −78.1 ± 1.5 mV (n = 18; P < 0.001) when rbE-II was co-expressed with β_1 (Fig. 3B).

The two most crucial characteristics with respect to the proposed physiological roles of LVA Ca^{2+} channels are that they will become available for opening (deinactivate) during the hyperpolarization that follows an action potential and that they will subsequently activate with small depolarizations. Although rbE-II meets both of these criteria, it is also apparent that it does not account for the properties of all LVA Ca^{2+} conductances. Compared to rbE-II,

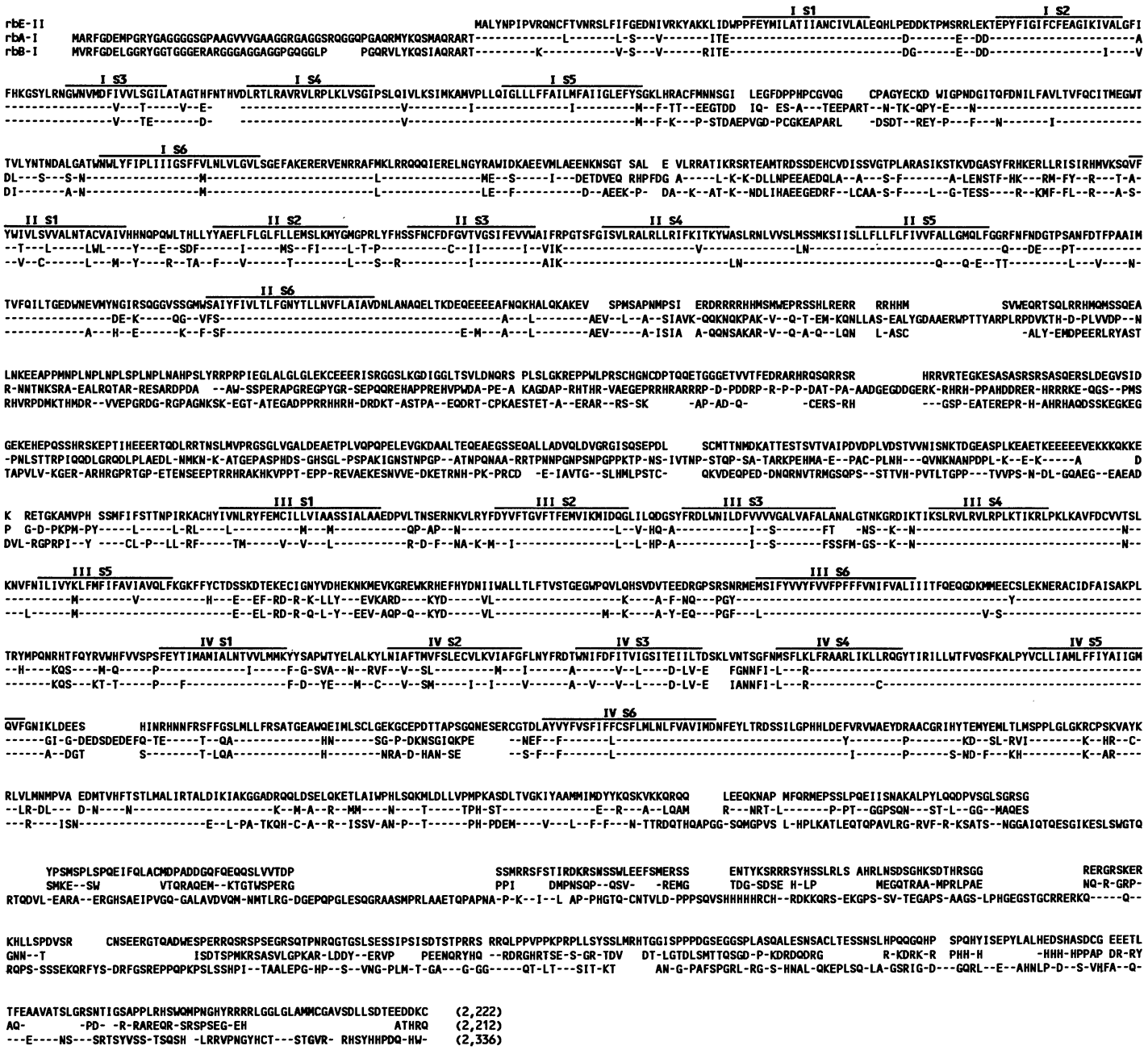

Fig. 1. The deduced amino acid sequence of the rbE-II protein (GenBank accession number L15453). The amino acid sequence of rbE-II is shown in single-letter code on the top of each line and is aligned with the rat brain class A (middle; rbA-I) and class B (bottom; rbB-I) α_1 subunits. Residues identical to rbE-II are shown as dashes, and gaps required to align the sequences are indicated by spaces. The four domains (I through IV) and putative transmembrane segments S1 through S6 are illustrated by horizontal bars. Abbreviations for the amino acid residues are: A, Ala; C, Cys; D, Asp; E, Glu; F, Phe; G, Gly; H, His; I, Ile; K, Lys; L, Leu; M, Met; N, Asn; P, Pro; Q, Gln; R, Arg; S, Ser; T, Thr; V, Val; W, Trp; and Y, Tyr.

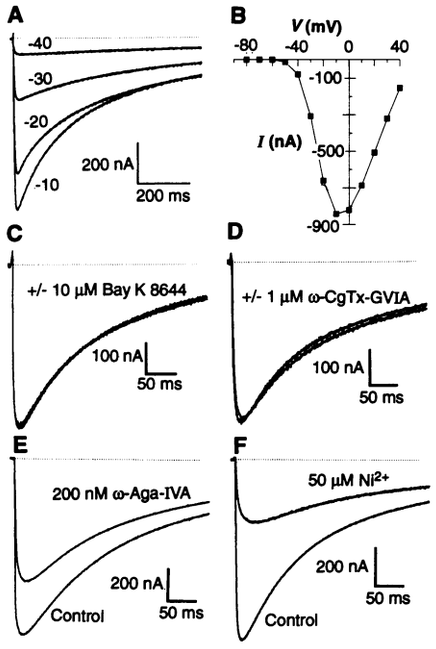

Fig. 2. Macroscopic properties and pharmacology of the rbE-II I_{Ba}. (**A**) Whole cell I_{Ba} of the rbE-II α_1 subunit alone. Shown is a family of current traces evoked from a holding potential of −100 mV to several test potentials (in millivolts). (**B**) Current-voltage relation of the rbE-II I_{Ba} measured from a holding potential of −100 mV. (**C**) Application of the L-type Ca^{2+} channel agonist Bay K 8644 (10 μM). (**D**) Exposure to the N-type Ca^{2+} channel antagonist ω-CgTx-GVIA (1 μM). (**E**) Exposure to the funnel-web spider peptide toxin ω-Aga-IVA (200 nM). (**F**) Blockade by 50 μM Ni^{2+}.

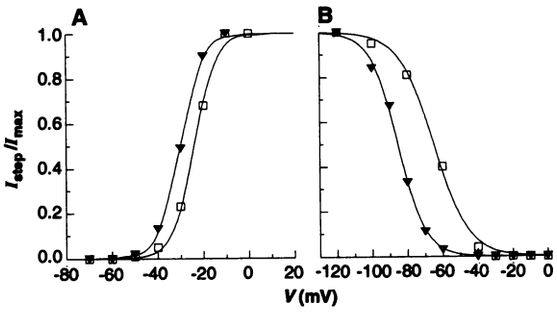

Fig. 3. Co-expression of rbE-II with the rat brain Ca^{2+} channel β_1 subunit. (**A**) Voltage dependence of activation of rbE-II (open squares) and rbE-II + β_1 (filled triangles). Currents were measured at a variety of test potentials (I_{step}) and were normalized to the maximum current (I_{max}). (**B**) Steady-state inactivation of rbE-II (open squares) and rbE-II + β_1 (filled triangles) I_{Ba}. Normalized I_{Ba} was determined by steps from various holding potentials (held for 20 s) to a test potential of 0 mV.

the prototypical T-type Ca^{2+} channel found in cardiac sinoatrial cells, sensory neurons, and endocrine cells activates and peaks at more hyperpolarized potentials and also inactivates at a faster rate (*2*, *6*). Similarly, the sensitivity of rbE-II to block by Cd^{2+} and its insensitivity to amiloride and octanol are also distinct from some LVA Ca^{2+} channels.

Northern (RNA) blot analysis showed that rbE-II was encoded by a major mRNA of ~12 kb expressed throughout the rat central nervous system. A more detailed analysis of rbE-II expression was performed with in situ hybridization with a ^{35}S-labeled complementary RNA probe (*16*). Large amounts of rbE-II transcripts were detected in periglomerular, mitral, and granule cells of the olfactory bulb (Fig. 4A), neocortical layers II through VI (Fig. 4, B through D), and entorhinal and piriform cortex (Fig. 4C). Expression was also noted in the striatum, lateral septum, and amygdala (Fig. 4B). In agreement with the PCR amplification of rbE-II from hippocampal RNA, very large amounts of rbE-II transcripts were seen in hippocampal pyramidal cells and the granule cells of the dentate gyrus (Fig. 4, B and C). In the hypothalamus, the supraoptic nucleus and the tuberal region showed large amounts of rbE-II transcripts (Fig. 4B). Expression in the thalamus was mainly localized to the intralaminar, parafascicular, and reticular nuclei (Fig. 4B). In addition, the rbE-II signal was particularly intense in the medial habenula (Fig. 4B). Transcripts were also noted in the substantia nigra pars compacta and the dorsal raphe (Fig. 4, C and D). In the caudal brain stem, high levels of expression were noted in the pontine nuclei (Fig. 4D), inferior olive, and the nucleus of the solitary tract (Fig. 4E). Within the cerebellar cortex, strong labeling was detected in the granule and Purkinje cell layers (Fig. 4E). Labeling was also detected in the pineal gland (Fig. 4D), the ganglion cell layer and inner nuclear layer of the retina, certain sensory ganglia, and the anterior and intermediate lobes of the pituitary. No labeling was detected in any of these structures with the use of a radiolabeled rbE-II sense probe (Fig. 4F).

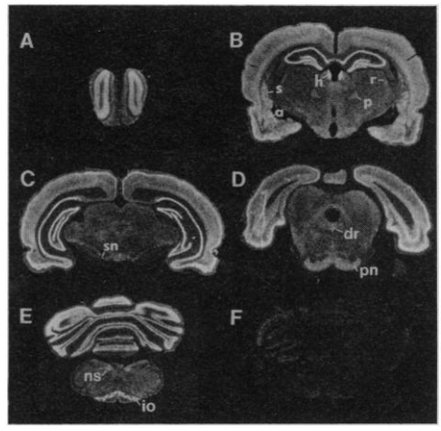

Fig. 4. In situ localization of rbE-II expressed in adult rat brain. Shown are dark-field images of coronal sections (rostral to caudal) with rbE-II localization with antisense (**A** to **E**) or sense (**F**) RNA probes (*16*). Abbreviations: a, amygdala; dr, dorsal raphe; h, medial habenula; io, inferior olive; ns, nucleus of solitary tract; p, parafascicular thalamus; pn, pontine nuclei; r, reticular nucleus of thalamus; s, striatum; sn, pars compacta of the substantia nigra. The slices were exposed for 6 days at −80°C.

Many of the cell types that express rbE-II have previously been shown to possess LVA Ca^{2+} conductances that may underlie the bursting properties of these neurons. Of particular note, Llinás and co-workers (*17*) first described LVA Ca^{2+} conductances that require hyperpolarization for repriming in the inferior olive and in the pars compacta of the substantia nigra. Low-threshold Ca^{2+} channels have also been proposed to underlie burst firing in the hippocampus, neocortex, dorsal raphe, and reticular nucleus of the thalamus (*18*). Two major subtypes of LVA Ca^{2+} currents have been described in different subsets of thalamic neurons (*19*). In a number of respects, the rbE-II I_{Ba} expressed in oocytes is similar to the LVA Ca^{2+} current, I_{TS}, found in the reticular nucleus cells and is distinct from the fast inactivating LVA Ca^{2+} current found in the relay nuclei of the thalamus (*19*).

It is becoming increasingly clear that as more cell types are examined in the mammalian central nervous system, Ca^{2+} channels that do not fit exactly into defined categories are being discovered. The diversity of properties described for LVA Ca^{2+} channels suggests that these channels are likely to be encoded by a heterogeneous family of proteins. In view of the structural similarities between rbE-II and cloned HVA Ca^{2+} channel α_1 subunits, our results suggest that this LVA Ca^{2+} channel shares a close evolutionary relation with the HVA Ca^{2+} channels. At the molecular level, the variability in LVA Ca^{2+} channels may be due to the existence of a gene family of α_1 subunits, alternative splicing, or the selective expression of ancillary proteins that differentially modulate α_1 subunit properties (for example, different β subunits). The cloning and functional expression of the rbE-II Ca^{2+} channel will aid in studies examining the roles of LVA Ca^{2+} channels in modulating firing patterns.

REFERENCES AND NOTES

1. R. J. Miller, *Science* 235, 46 (1987); R. Llinás, *ibid.* 242, 1654 (1988).
2. R. W. Tsien, D. Lipscombe, D. V. Madison, K. R.

Bley, A. P. Fox, *Trends Neurosci.* **11**, 431 (1988); B. P. Bean, *Annu. Rev. Physiol.* **51**, 367 (1989); P. Hess, *Annu. Rev. Neurosci.* **13**, 337 (1990).
3. K. P. Campbell, A. T. Leung, A. H. Sharp, *Trends Neurosci.* **11**, 425 (1988); W. A. Catterall, M. J. Seagar, M. Takahashi, *J. Biol. Chem.* **263**, 3535 (1988); M. W. McEnery *et al.*, *Proc. Natl. Acad. Sci. U.S.A.* **88**, 11095 (1991).
4. R. W. Tsien, P. T. Ellinor, W. A. Horne, *Trends Pharmacol. Sci.* **12**, 349 (1991); T. P. Snutch and P. B. Reiner, *Curr. Opin. Neurobiol.* **2**, 247 (1992).
5. A. Mikami *et al.*, *Nature* **340**, 230 (1989); M. Biel *et al.*, *FEBS Lett.* **269**, 409 (1990); M. E. Williams *et al.*, *Neuron* **8**, 71 (1992); M. E. Williams *et al.*, *Science* **257**, 389 (1992); Y. Mori *et al.*, *Nature* **350**, 398 (1991).
6. E. Carbone and H. D. Lux, *Nature* **310**, 501 (1984); B. P. Bean, *J. Gen. Physiol.* **86**, 1 (1985); C. M. Armstrong and D. R. Matteson, *Science* **227**, 65 (1985); M. C. Nowycky, A. P. Fox, R. W. Tsien, *Nature* **316**, 440 (1985); A. P. Fox, M. C. Nowycky, R. W. Tsien, *J. Physiol.* (*London*) **394**, 149 (1987).
7. M. Steriade and R. R. Llinás, *Physiol. Rev.* **68**, 649 (1988).
8. D. A. Coulter, J. R. Huguenard, D. A. Prince, *Neurosci. Lett.* **98**, 74 (1989).
9. Total cellular RNA isolated from adult rat hippocampus was amplified with PCR and degenerate oligonucleotides that recognize the highly conserved region, domain IV S5 to just past domain IV S6 in cloned Ca^{2+} channel α_1 subunits. Examination of 16 separate subcloned PCR products showed that 13 corresponded to previously identified rat brain Ca^{2+} α_1 subunits, whereas three encoded a new class of α_1 subunit (class E). Two class E cDNAs, rbE-123 (6249 bp) and rbE-2 (5366 bp), were isolated by screening a rat brain cDNA library. The rbE-123 and rbE-2 DNA sequences overlap by ~4.1 kb and together encode the entire rbE α_1 subunit protein (designated rbE-II). The rbE-II protein is ~93% identical to the rabbit brain BII Ca^{2+} channel sequence recently reported [T. Niidome, M.-S. Kim, T. Friedrich, Y. Mori, *FEBS Lett.* **308**, 7 (1992)].
10. T. P. Snutch, W. J. Tomlinson, J. P. Leonard, M. M. Gilbert, *Neuron* **7**, 45 (1991); T. V. B. Starr, W. Prystay, T. P. Snutch, *Proc. Natl. Acad. Sci. U.S.A.* **88**, 5621 (1991); S. J. Dubel *et al.*, *ibid.* **89**, 5058 (1992).
11. For expression studies, the full-length rbE-II cDNA was subcloned into the vertebrate expression vector pMT2 (Genetics Institute, Cambridge, MA), and macroscopic currents were recorded 2 to 5 days after nuclear injection of the rbE-II construct (~1 ng) into *Xenopus laevis* oocytes. Barium saline contained 4 mM $BaCl_2$, 38 mM KCl, 36 mM tetraethylammonium chloride, 5 mM 4-aminopyridine, 0.4 mM niflumic acid, and 5 mM Hepes (pH 7.5). In some cells, the rbE-II I_{Ba} appeared to run down (almost 50% in 2 to 3 min) during normal recording. Only those currents that showed little or no rundown were used in the pharmacology experiments. In uninjected control oocytes, the endogenous I_{Ba} averaged ~4 nA (n = 18). All currents were leak- and capacitance-subtracted and filtered at 1000 Hz.
12. To confirm that rbE-II activated at hyperpolarized potentials relative to HVA Ca^{2+} channels, we compared the properties of rbE-II to cloned rat brain class B (N-type) and class C (L-type) Ca^{2+} channel α_1 subunits (*10*). Activation curves fitted to normalized currents (measured in 40 mM Ba^{2+} saline) showed that $V_{1/2}$ for rbE-II was -16.1 ± 1.4 mV (n = 9) compared with -0.8 ± 1.3 mV (n = 11) and 4.3 ± 1.8 mV (n = 10) for the class B and class C α_1 subunits, respectively.
13. I. M. Mintz, M. E. Adams, B. P. Bean, *Neuron* **9**, 85 (1992).
14. A. E. Lacerda *et al.*, *Nature* **352**, 527 (1991); X. Wei *et al.*, *J. Biol. Chem.* **266**, 21943 (1991); D. Singer *et al.*, *Science* **253**, 1553 (1991).
15. For nuclear injections, the rat brain β_1 subunit [M. Pragnell, J. Sakamoto, S. D. Jay, K. P. Campbell, *FEBS Lett.* **291**, 253 (1991)] was subcloned into pMT2. In control oocytes injected with the β_1 subunit alone, the endogenous I_{Ba} was 25.0 ± 5.6 nA (n = 12).
16. In situ localization was performed with 30-μm fixed sections from 250- to 300-g adult male rat brains. Sense and antisense ^{35}S-labeled RNA probes were synthesized from a 359-bp template derived from the domain II to III loop of rbE-II. After the films were developed, some sections were dipped in emulsion (Kodak, NTB-2) and exposed for 2 weeks at 4°C.
17. R. Llinás and Y. Yarom, *J. Physiol.* (*London*) **315**, 549 (1981); *ibid.*, p. 569; *ibid.* **376**, 163 (1986); R. Llinás, S. A. Greenfield, H. Jahnsen, *Brain Res.* **294**, 127 (1984).
18. R. K. S. Wong and D. A. Prince, *Brain Res.* **159**, 385 (1978); A. Friedman and M. J. Gutnick, *Neurosci. Lett.* **81**, 117 (1987); R. J. Sayer, P. C. Schwindt, W. E. Crill, *ibid.* **120**, 175 (1990); T. M. Burlhis and G. K. Aghajanian, *Synapse* **1**, 582 (1987); D. A. Coulter, J. R. Huguenard, D. A. Prince, *J. Physiol.* (*London*) **414**, 587 (1989).
19. J. R. Huguenard and D. A. Prince, *J. Neurosci.* **12**, 3804 (1992).
20. We thank M. Gilbert, E. Mathews, and P. Reiner for their comments on the manuscript, M. Adams for generously providing the ω-Aga-IVA, and K. Campbell and M. Pragnell for the rat brain β_1 subunit. Supported by grants from the Medical Research Council of Canada (T.P.S. and S.R.V.), the British Columbia Health Care Research Foundation (S.R.V.), and the Howard Hughes Medical Institute International Research Scholars Program (T.P.S.). T.W.S. is supported by a postdoctoral fellowship and is on leave from the Institute of Molecular and Cell Biology, National University of Singapore, and A.S. is supported by a postdoctoral fellowship from the Natural Sciences and Engineering Research Council of Canada. S.R.V. is a Medical Research Council scientist, and T.P.S. is the recipient of a research fellowship from the Alfred P. Sloan Foundation.

24 February 1993; accepted 28 April 1993